Selective Removal of Hg^{2+} Ions from Water Using New Functionalized Silica Resin: Equilibrium, Thermodynamics and Kinetic Modeling Studies

[1]Nida Shams Jalbani, [1]Amber R Solangi*, [1]Shahabuddin Memon, [1]Ranjhan Junejo, [2]Asif Ali Bhatti
[1]*National Center of Excellence in Analytical Chemistry, University of Sindh, Jamshoro-76080 / Pakistan.*
[2]*Department of Chemistry, Government College University Hyderabad, Hyderabad, 71000, Pakistan.*
ambersolangi@gmail.com*

(Received on 10th November 2020, accepted in revised form 3rd February 2021)

Summary: In current study, the diphenylaminomethylcalix[4]arene (**3**) was synthesized and immobilized onto silica surface to prepare a selective, regenerable and stable resin-4. The synthesized resin-4 has been characterized by FT-IR spectroscopy, scanning electron microscopy, energy-dispersive X-ray spectroscopy (EDX) and Brunauer-Emmett-Teller (BET) techniques. To check the adsorption capacity of resin-4, the batch and column adsorption methodology were applied and it has observed that the resin-4 was selectively removed Hg^{2+} ions under the optimized parameters. The maximum adsorption capacity was obtained at pH 9 using 25 mg/L of resin-4. Under the optimal conditions, different equilibrium, kinetic and thermodynamic models were applied to experimental data. The results show that adsorption mechanism is chemical in nature following Langmuir model with good correlation coefficient (R^2=*0.999*) and having 712.098 (mmol/g) adsorption capacity. The energy of calculated from D-R model suggests the ion exchange nature of the adsorption phenomenon. Dynamic adsorption experiments were conducted using Thomas model. The maximum solid phase concentration (*qo*) was 7.5 and rate constant k_{TH} was found to be 0.176 with (R^2=0.938) for Hg^{2+} ions. The kinetic study describes that the adsorption mechanism follows pseudo second order (R^2=0.999). The thermodynamic parameters such as ΔH (0.032 KJ/mol) and ΔS (0.127 KJ/mol /K) and ΔG (-5.747,-6.306, -7.027 KJ/mol) shows that the adsorption of Hg^{2+} ion is endothermic and spontaneous. The reusability of resin-4 was also checked and it has observed that the after 15 cycle only 1.2 % adsorption reduces. Moreover, the resin-4 was applied on real wastewater samples obtained from local industrial zone of Karachi, Sindh-Pakistan.

Keywords*:* Calix[4]arene based silica resin, Metal ion, Batch and column adsorption, Toxic pollutant, Adsorption of mercury, Thermodynamic and kinetic modeling.

Introduction

In recent, rapid development in science and technology as well as in industrial sector have taken human being to next level, but on other side, its negative effect on ecosystem caused severe human health risk [1-3]. Water is most important component of life, without water life is impossible. Clean and pure water is everyday need of living things. Water infected by industrial waste flow of hazardous and toxic substances is serious issue worldwide [4, 5]. Among pollutants, toxic metal ions present in very low concentration have harmful impact on human health [6-8]. Mercury is one of the most toxic metal ion released from industrial waste into natural water sources without proper treatment. It mainly occurs in elemental mercury (Hg°), inorganic mercury (Hg^{+}, Hg^{2+}) and organic mercury such as methyl mercury which is more toxic as compared to other states of mercury and inorganic mercury [9, 10]. Different world agencies have provided permissible level of mercury in drinking water, for instance, WHO has allowed 1µg/L, EPA has allowed 2µg/L, while the EU allowed maximum level 0.07 µg/L [11]. It produce toxic effects which are major cause of lung cancer, bladder, kidney failure diseases [12, 13]. Therefore, it is necessary to eliminate this toxic metal ion from waste water at very low concentration before release to natural water sources. Presently, there are different available strategies for the removal of mercury such as coagulation, on-line dialysis ion exchange chromatography, adsorption, chemical precipitation, electrolytic process, solvent extraction and reverse osmosis. Among these techniques, adsorption is most efficient, low cost and simple technique [14-18]. In adsorption techniques, natural and synthetic materials are used, but it is important that the adsorbent should be stable under the thermal and chemical conditions and has wide pH range along with high adsorption capacity.

Currently, different organic and inorganic based polymeric materials are applied for the treatment wastewater, while the immobilization of organic functional groups or ligands onto inorganic polymeric matrices produce modified adsorbent attracts much attention regarding their selectivities and high adsorption capacities as compared to previously used materials [19]. Silica gel is most commonly used inorganic adsorbent for the adsorption of metal ions and the silanol groups present on its surface are weak ion exchanger and has very less selectivity and adsorption capacities over wide range of the pH. Therefore, many studies were performed for the modification of silica surface with organic moieties through chemical bonding with silica-silanol to prepare the selective, stable and high adsorption capacity material for the treatment of wastewater

*To whom all correspondence should be addressed.

effluents [20, 21]. Previously, many adsorbents have been prepared by immobilization of different organic moieties onto silica but recently the third generation in supramolecular compounds such as calixarenes are also used as a functional material for the immobilization purpose. Basically, the calixarenes are cyclic oligomers and these ionophores have unlimited derivatization such as amines, amides, carbonyls, nitriles and other suitable moieties that can bind to metal ions, anions and neutral molecules [22-25]. Furthermore, the immobilization of calix[n]arene derivatives onto silica gel increases the reusability as well selectivity of adsorbent and enhance the adsorption capacities. In previous studies, many materials have been reported based on immobilization of calix[n]arene moieties onto silica gel. In literature, the study has been reported using p-piperdinomethylcalix[4]arene immobilized silica resin for the online-solid phase extraction of metal ions from water which demonstrate that the prepared resin was selective for Cu^{2+} and Pb^{2+} metal ions among the other ions [26]. Another study has been reported based on functionalized calix[4]arene silica resin for the treatment of metal contaminated wastewater, which demonstrate the resin was selective for Cd^{2+}, Pb^{2+}, and Hg^{2+} metal ions [27].

In this study, the *p*-diphenylaminomethylcalix[4]arene calix[4]arene has been synthesized and immobilized onto silica surface and applied onto water samples. This resin shows the selectivity towards Hg^{2+} ions only in presence of other metal ions of the same charge and has good stability and efficiency after using many cycles.

Experimental

Chemicals and Reagent

The chemicals used in this study were analytical grade, supplied by different chemical supplier companies such as Toluene, Chloroform, Dichloromethane and Tetrahydrofuran THF have been provided by Merck. 4-tert: butyl phenol was purchased Alfa Aesar 99%. Formalin was purchased from sigma Aldrich. The silica gel (230–400 mesh) was procured from Sigma Aldrich.

Instrumentation

The synthesized material has been characterized by Elemental analyses, FTIR spectroscopy, and surface analyzing techniques such as BET, EDX and SEM. The FTIR spectroscopy have been performed for all synthesized compounds by using Thermo Nicollet 5700 FT-IR spectrometer (WI. 53711, USA). The surface of resin-4 was characterized by SEM (JSM-6380) model instrument. The surface area, pore size and pore volume of synthesized material have been analyzed by Quanta chrome® ASiQwin™ surface area analyzer. The metal concentration was determined by using atomic absorption spectrophotometer (Perkin Elmer model Analyst 700; Norwalk, CT, USA). The pH of the solution was adjusted by 0.1 M NaOH/HCl using wtw pH meter.

Synthesis

The compound **1**-**3** have been synthesized by previously reported methods. While the synthesis of compound **4** was performed by reported procedures after modification [19, 28]. All compounds were characterized by FT-IR, EDX and SEM techniques.

Synthesis of Resin-4

In a flask, 8g of silica was weighed and washed with dilute HCl and deionized water and dried in oven at for 3h. After drying, 250 mL $SiCl_4$ (0.1 M) in pre-dried CH_2Cl_2 was added into silica powder along with the addition of 3 mL triethylamine ($C_6H_{15}N$), resulted in a cloudy mixture formed and kept for overnight. The remaining solvent was removed by using a rotatory evaporator. After removing the solvent from silica, added 1.5g diphenylaminomethylcalix[4]arene (**3**) into it, which was already dissolved in 30 mL Chloroform. The reaction was started to reflux followed by the addition of some drops of triethylamine. The reaction mixture was monitored with the passage of time by using FTIR spectroscopy technique. After completion of reaction, the synthesized product has been filtered and unreacted other materials have been washed by $CHCl_3$, CH_3OH, H_2O and finally $CHCl_3$. The gravimetric method of analysis was performed to check the amount of derivative attached to the silica surface and it has found to be 0.68×10^{-4} mmol g^{-1}.

Adsorption Procedure

Batch Method

Static/batch method of adsorption have been performed to check the ability of resin-4 for the removal of metal ions. The (10 mL 1×10^{-4} M) solution of metal nitrates were taken into Erlenmeyer flask and 25 mg/L of resin-4 was added and placed onto mechanical shaker for 60 minutes. The resin-4 was filtered off and remaining concentration of metal ions were determined by atomic absorption spectrophotometer (*AAS*). The real wastewater samples were collected from local industrial zone of Karachi Sindh-Pakistan. The % removal or adsorption and adsorption capacity were determined using following equations 1 and 2:

$$\% \ adsorption = \frac{C_i - C_f}{C_i} \times 100 \quad (1)$$

$$q_e = \frac{(C_i - C_e)V}{m} \quad (2)$$

In equation 1 C_i and C_f (mol/ L) are the initial and final concentration respectively. In equation 2 q_e (mg/g) is the adsorption capacity, while the C_i and C_e is the initial and equilibrium concentration respectively, V is the volume (mL) of solution and m is the mass of resin-4.

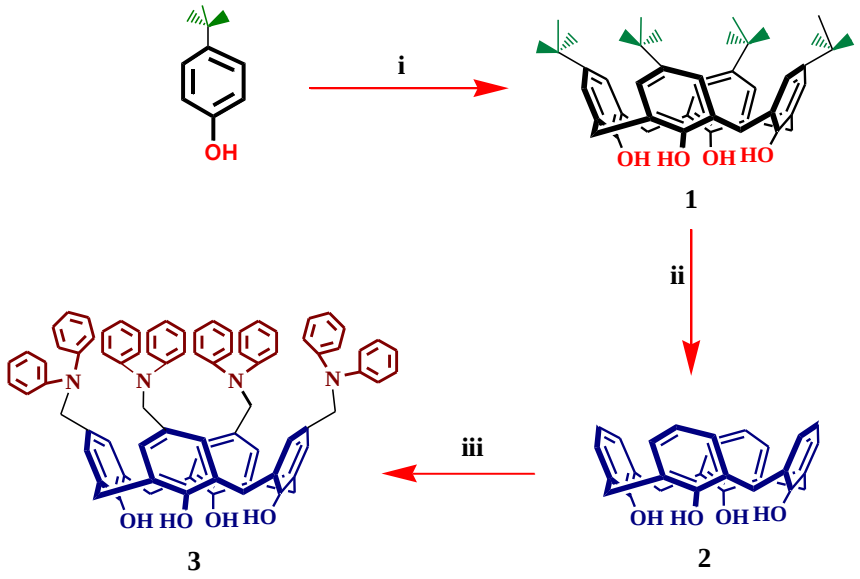

Scheme.1: Synthesis of *p*-diphenylaminomethylcalix[4]arene (i) HCHO/NaOH (ii) $AlCl_3$/Phenol (iii) Diphenylamine/HCHO/CH_3COOH.

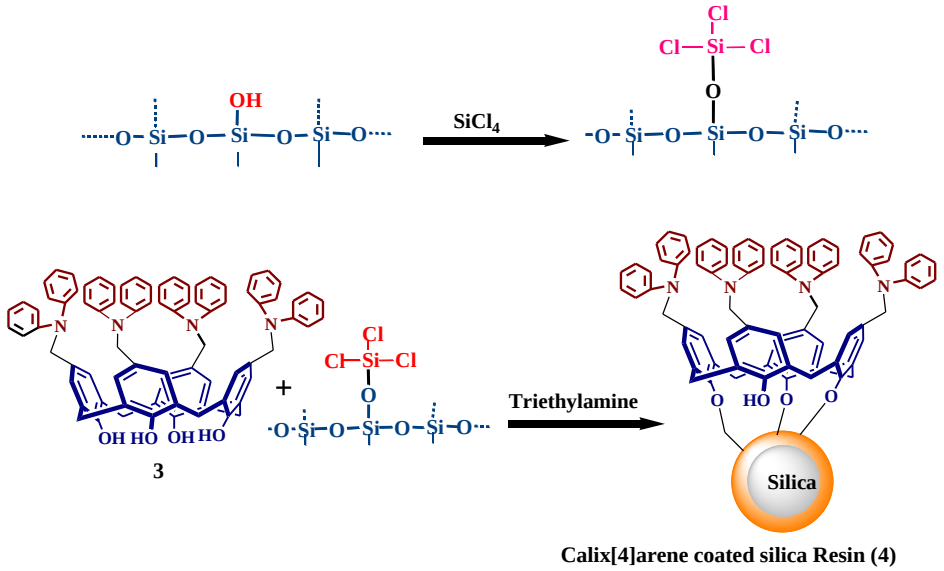

Calix[4]arene coated silica Resin (4)

Scheme.2: Schematic route for the synthesis of resin-4.

Column Adsorption

The column study was performed using a plastic syringe column with 1 cm inner diameter and a 6 cm height filled up to 1 cm with resin-4. The bottom of the column was plugged in with glass wool just to make a support for the resin-4 to prevent its floating from the outlet. The column was packed by loading 150 mg of resin-4. The metal solution of Hg^{2+} with 1×10^{-4} M concentration with flow rate 2 mL/min was adjusted. This process was continued until the column gets exhausted and the concentration of Hg^{2+} ion was analysed by *AAS* spectrophotometer.

Thomas Model

The break through curve can be obtained by plotting the graph between (C_t/C_i) vs time. The column with better removal capacity can be designed with the help of breakthrough profiles. The experimental data have been analyzed by Thomas model and from the linear equation the (q_o) and (k_{TH}) have been calculated. The value of (q_o) describes the solid-phase concentration while (k_{TH} shows the Thomas rate constant. The values were obtained by plotting the graph $\ln\left(\frac{Co}{C}-1\right)$ against t while the flow rate remains constant.

$$\left(\ln\frac{Co}{C}-1\right)=\frac{k_{TH}q_oA}{Q}-\frac{k_{TH}C_i}{Q}V_{eff} \qquad (3)$$

Here, *Co* (mol/L) is the initial and *C* (mol/L) is the effluents concentration. The *Q* describes the flow rate ($mLmin^{-1}$) *A* is the adsorbed quantity of metal ion.

Results and Discussion

Adsorption of Hg^{2+} ions onto Resin-4

The adsorption of Hg^{2+} ions onto resin-4 takes place through the formation of metal ion complexation with amine moieties of resin-4. The electron donating nature of amine group and electron accepting nature of metal ions creates the ionic interaction. These electronic interaction are favorable for trapping the metal ions with their soft binding sites. To check the metal ions complexation with resin-4 different analytical procedures were applied and it has observed that the resin-4 has higher binding capacity for Hg^{2+} ions. Moreover, the amine groups present onto resin-4 are soft mannich bases as compared to other hard groups which may prefer to hard metal ions. Thus, the interaction results of Hg^{2+} ions and resin-4 confer to follow the Pearson's 'hard and soft acids and bases' concept [29] due to the soft sites of amine groups has high attraction for Hg^{2+} metal ions. The proposed interaction of resin-4 with Hg^{2+} ions is shown in Fig. 1.

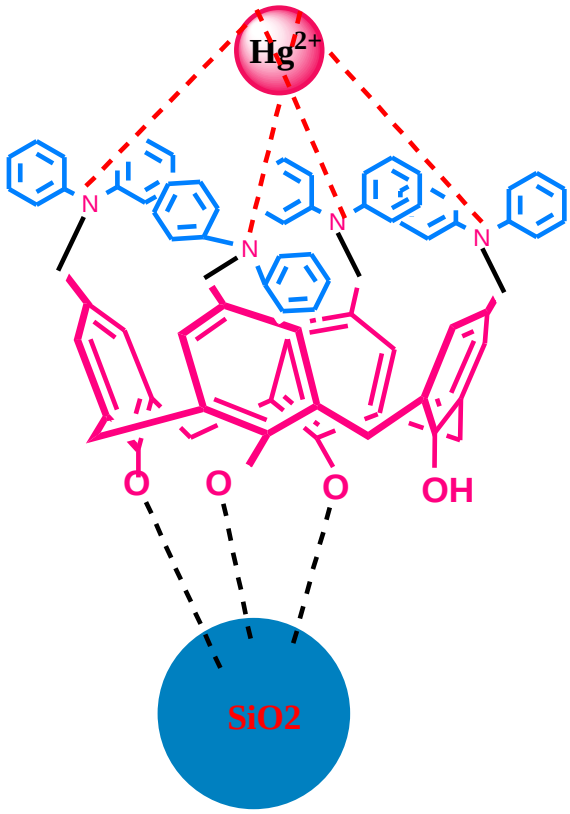

Fig.1: Representation of proposed interaction between resin-4 and Hg^{2+} ion.

FTIR Spectroscopy

All the synthesized compounds were characterized by FTIR spectroscopy, given in Fig.2. In Fig 2 spectrum (a) is of pure silica which has characteristic peaks at 3454, 1637 cm^{-1} for OH, Si-O stretching respectively while 1093 cm^{-1} is the OH bending frequency. The spectrum (b) is of diphenylaminomethylcalix[4]arene characterized by the strong absorbance at 3392, 2921,1593 cm^{-1} due to O-H, C-H and C-O stretching frequencies respectively. The peak observed 1448 cm^{-1} is O-H bending. The peaks at 1473 and 1240 cm^{-1} are the characteristic peaks for C-O and C-N stretching frequencies respectively. The spectrum (c) is of resin 4 which shows some new bands at 3490, 2950, 1610 and 1384 cm^{-1} are the peaks for OH, C-H, C-O, C-N stretching frequencies while the 1093cm^{-1} is OH bending frequency. These peaks confirms the attachment of compound **3** onto silica. The spectrum (d)

is resin-4 after loading the Hg^{2+} ions which shows the disappearance of C-N stretching peak. Previously, different resin have been performed and confirmed through FT-IR technique. For example diethylamine functionalized calix[4]arene immobilized onto silica surface was confirmed by FT-IR spectroscopy. The resin have different new addition peaks compared to pure silica [27]. Another study was performed for the removal of azo dyes using the sulphonate calix[8]arene attached silica resin. The attachment of sulphonate calix[8]arene onto silica was confirmed through FT-IR technique in which resin have some new peaks after immobilization [23]. Herein, the diphenylaminomethylcalix[4]arene was immobilized onto silica surface and confirmed by FT-IR spectroscopy technique.

Characterization of Resin-4 by Scanning Electron Microscopy (SEM)

The synthesized resin-4 was characterized by SEM technique. SEM technique is very helpful to characterize the surface morphology of materials. In this regard, the image (a) is of pure silica which shows very clear surface and crystalline structure of material. While the image (b) is of resin-4 which is prepared by immobilization of compound **3** onto silica, which has very rough surface and amorphous. The roughness is of attachment of compound **3** onto silica. In the literature, the immobilization of calix[4]arene based ligands onto silica surface have been characterized by SEM technique such as p-piperdinomthylcalix[4]arene ligand immobilized onto silica surface and characterized by SEM technique [30, 31]. In this study, the diphenylaminomethylcalix[4]arene immobilized onto silica surface was characterized by SEM technique Fig 3.

Characterization of Resin-4 by EDX Technique

The energy-dispersive X-ray spectroscopy is a technique used to show the chemical composition of material. Therefore, the resin-4 has been analyzed by EDX technique. The results shown in Fig 4 demonstrate the presence of carbon (C), oxygen (O) and silicon (Si). The atomic percentage (wt%) of all elements present were calculated after the modification of silica in following order C (39.4%), O (61.3%) and Si (41%). In the same way, the percentage (wt%) of all elements was investigated as: C (38%), O (44%) and Si (17%).

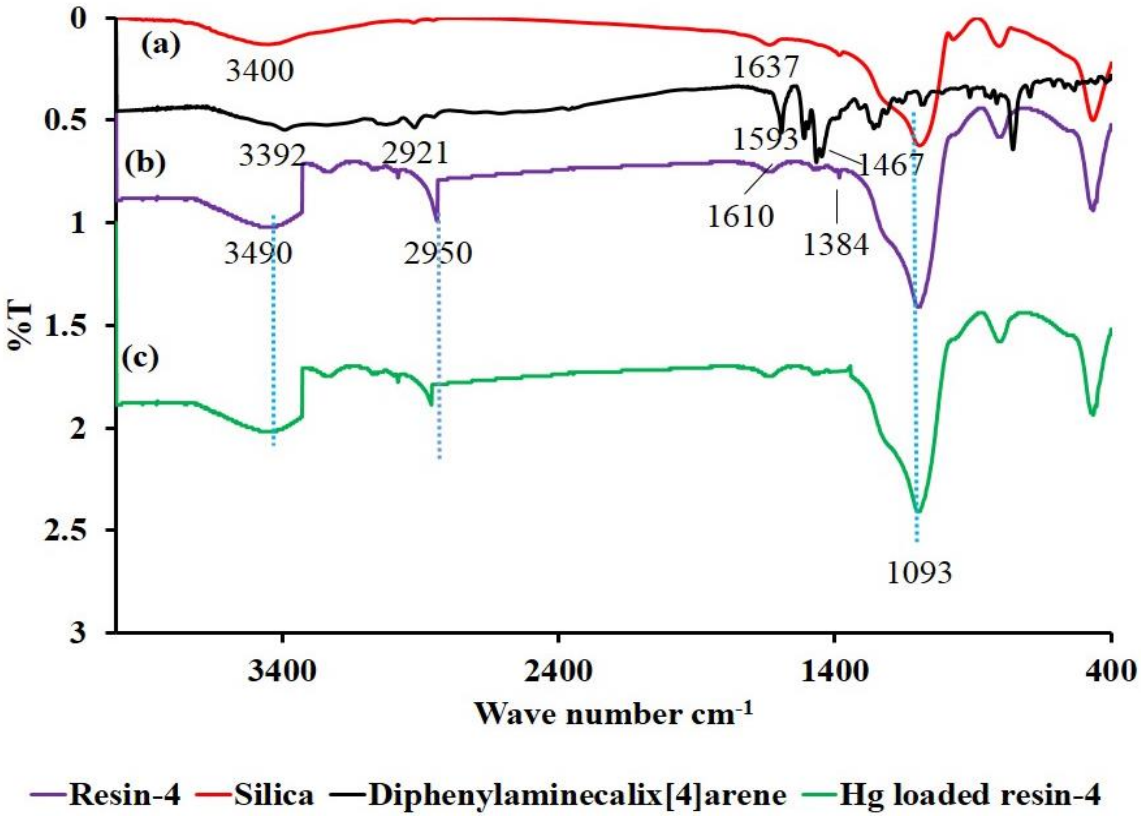

Fig. 2: The FT-IR characterization of synthesized compounds. The spectrum (a) is of pure silica (b) is of *p*-diphenylaminomethylcalix[4]arene (c) resin-4 (d) is the loaded of Hg^{2+} ions onto resin-4.

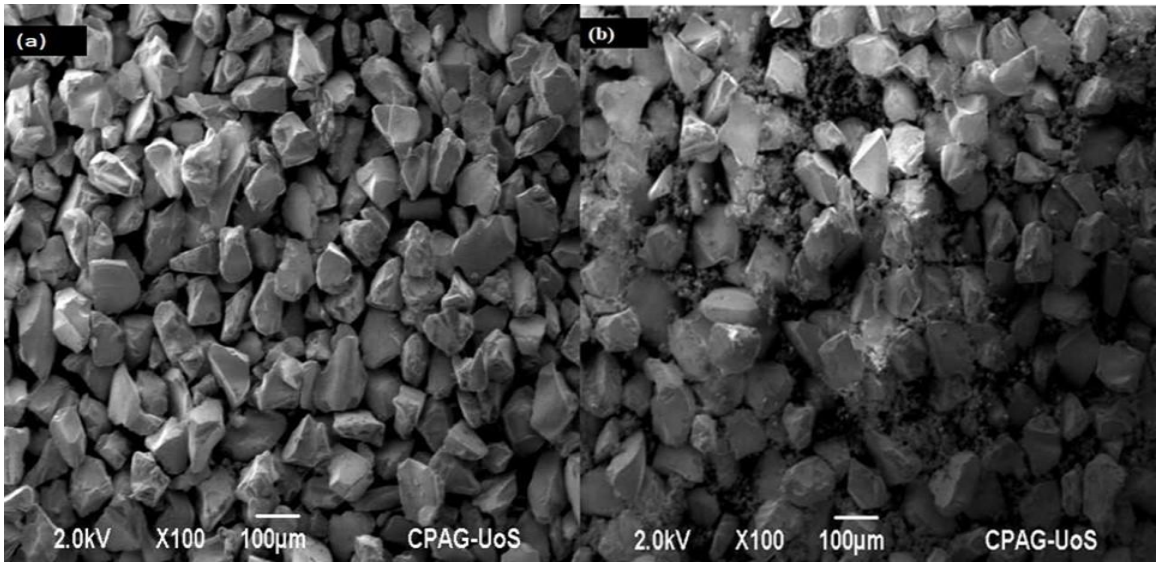

Fig.3: The SEM monographs, image (a) of silica (b) of resin-4.

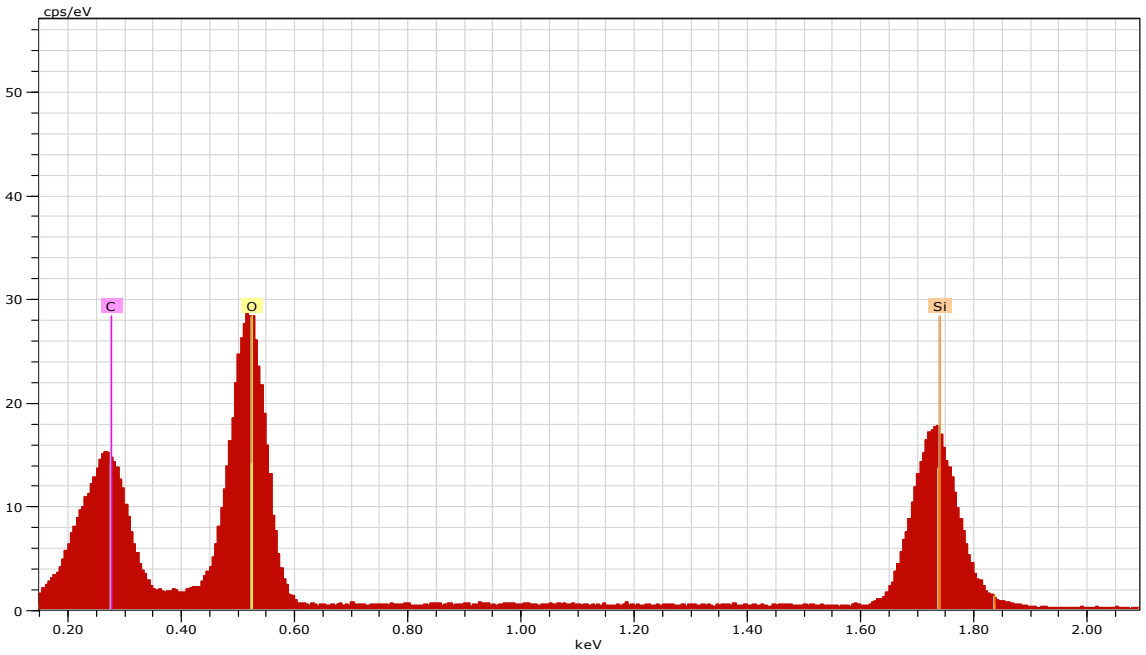

Fig.4: The EDX spectrum of resin-4.

Characterization of Resin-4 by BET Technique

The Brunauer-Emmett-Teller (BET) technique is helpful for the analysis of materials surface area by multilayer nitrogen adsorption as a function of relative pressure shown in Fig 5. The adsorption and desorption isotherm clearly shows that it is type IV isotherm according to IUPAC classification. The pore area and total specific surface area in m^2/g have been determined using BJH methods as shown in below in Fig 5.

Metal Ions Selectivity by Resin-4

The synthesized resin-4 have been applied in batch adsorption to check the selectivity and efficiency of resin. Therefore, the solution of metal nitrates with (1×10^{-4} mol/L) concentration and 25 mg/L of resin-4 have been examined and mentioned in Fig 6. The result shows that the resin-4 has good ability for Hg^{2+} ions among the various metal ions. Other metal ions remain

less selective as compared to Hg^{2+} ions. This may be due to ionic size and charge of mercury ions. Moreover, the binding sites present on resin-4 are soft and softness of metal ions also contributes to the complexation between resin-surface and metal ion. The resin-4 has nitrogen group that are soft mannich bases which may prefers the mercury ions over the other metal ions because of their borderline softness nature compared to other ions in solution.

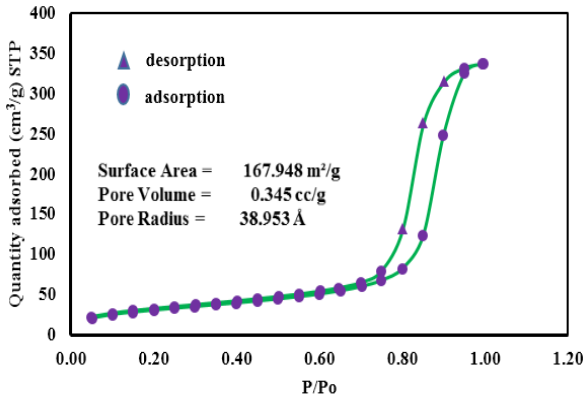

Fig.5: Nitrogen adsorption−desorption isotherm plots of resin-4**.**

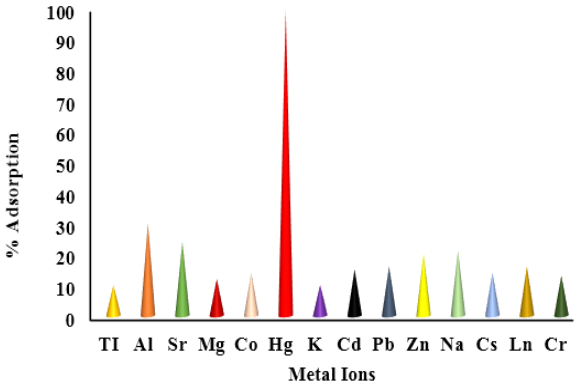

Fig.6: The Adsorption (%) of different metal ion onto resin-4. (10 mL of Hg^{2+} ions solution (1×10^{-4} mol/L) 60 min contact time at 298 K).

Dosage Effect of Resin-4

The effect of resin-4 dosage on % adsorption of Hg^{2+} ions were performed by using different amounts of resin-4 ranging from 10 to 55 mg/L at constant concentration (1×10^{-4} mol/L). The % adsorption increased with the addition of resin-4. The maximum % adsorption was achieved at 25 mg/L i.e 92% while dosage more than 25 mg/L shows no significant change in the % adsorption Fig 7a.

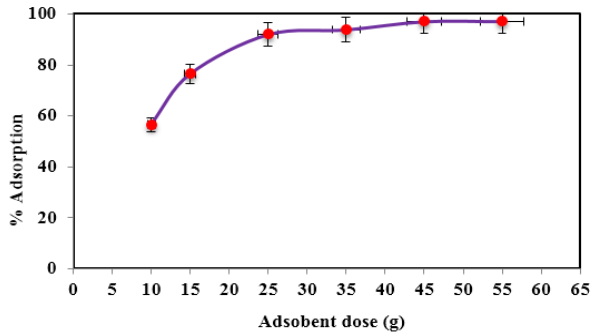

Fig.7a: Effect of resin-4 dosage on % adsorption of Hg^{2+} ions (1×10^{-4} mol/L) 60 min contact time at 298 K).

Effect of pH

The pH of the solution is most important parameter in adsorption. To study the influence of pH onto resin-4, the batch adsorptions studies have been performed ranging from 3–10.5 at the fixed concentration and resin-4 dosage. The results show that the adsorption of Hg^{2+} ions takes place at basic medium as compared to acidic solution i.e. pH 9.0. The high adsorption percentage of Hg^{2+}ions at specific pH values describes the importance of resin-4 to be utilized for the treatment of Hg^{2+} ions contaminated water. The effective removal of Hg^{2+} ions through resin-4 at basic pH is due to the presence of amine functionality. At the acidic pH the protonation of amine takes place that may produce electrostatic repulsion between the Hg^{2+} ions and protonated amines. However at basic media the strong electrostatic attraction takes place between amine and metal cation which enhance the adsorption capacity of resin-4**.** Therefore, all the experimental studies were performed at pH 9.

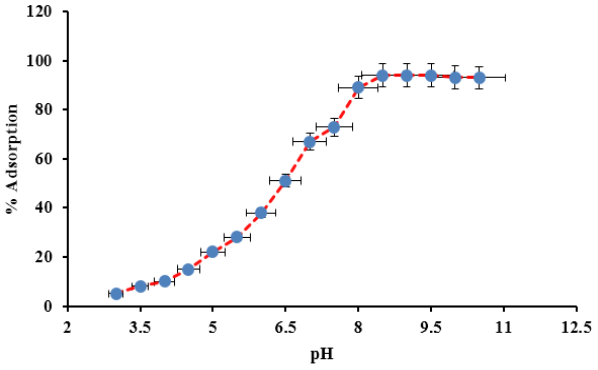

Fig.7b: Effect of pH on % adsorption of Hg^{2+} ions (25 mg/L of resin-4, 1×10^{-4} mol/L 60 min contact time, at 298 K).

Adsorption Isotherms Models

The adsorption phenomenon can be defined very well by adsorption isotherms, which describes the quantity of adsorbate adsorbed onto certain amount of adsorbent at specific temperature. In adsorption modeling, the equilibrium concentrations were applied at constant temperature. To remove the toxicants from wastewater, the equilibrium system was validate using isotherm models to check the monolayer or multilayer surface formation and mechanism of adsorption either ion exchange, chemical or physical in nature [32].

Langmuir equilibrium model describes the monolayer formation of Hg^{2+} ions onto resin-4 surface and binding energy of the adsorption is a constant value. The Langmuir model can be calculated using equation 4, in which the initial concentration of Hg^{2+} ions solution optimized from (1×10^{-4} to 1×10^{-7}) mol/L with the 25mg/L amount of resin-4 with 60 min of equilibrium time. The adsorption capacity Q (mmol/g) of Hg^{2+} ions from aqueous media to the resin-4 surface is given in Table-1 obtained by plotting the graph between C_e/C_{ad} versus C_e as shown in Fig 8. The value of (R^2=0.999) shows the linearity and fitness of this model for the adsorption of Hg^{2+} ions onto resin-4.

$$\left(\frac{C_e}{C_{ads}}\right)=\left(\frac{1}{Qb}\right)+\left(\frac{C_e}{Q}\right) \qquad (4)$$

In equation 4, the C_{ads} is the adsorbed metal ion concentration and C_e is the metal ion equilibrium concentration while Q is the maximum amount of solute adsorbed at monolayer formed surface.

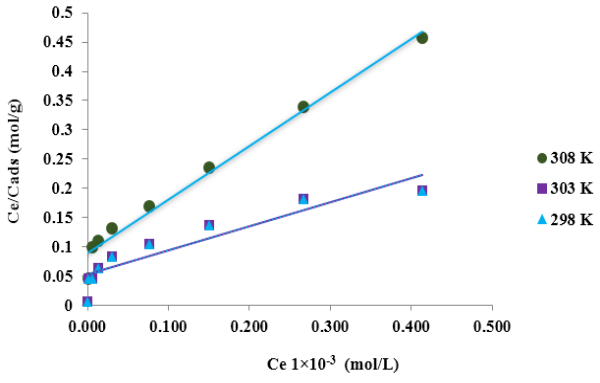

Fig.8: Langmuir isotherm model (Conc. 1×10^{-7} to 1×10^{-4} mol/L, 25 mg/L resin-4**,** 60 min shaking time at 9 pH and 298-308 K).

The R_L is an equilibrium parameter known as separation factor which is a dimensionless constant and used to characterize the feasibility Langmuir model. The R_L value can be calculated with the help of equation (5).

$$R_L=\frac{1}{(1+bC_i)} \qquad (5)$$

Here b shows the Langmuir constant and C_i (mol/L) is the initial concentration. The value of R_L describes the type of isotherm i.e if R_L = 0: the isotherm is known as irreversible isotherm, while the value is in range of 0 < R_L < 1: this is known as favorable isotherm and R_L value =1: is a linear isotherm and greater 1 is unfavorable isotherm model.

Table-1: Langmuir adsorption isotherm parameters.

Temperature	*Q* (mmol/g)	*b*	R_L	R^2
298	711.892	15.07	0.95-0.821	0.989
303	712.031	15.45	0.80-0.781	0.990
308	712.098	16.13	0.91-0.931	0.999

The Freundlich isotherm model explains the multilayer formation on adsorbent surface. The equilibrium data was applied by Freundlich model using equation (6).

$$\log C_{ads}=\log A+\left(\frac{1}{n}\right)\log C_e \qquad (6)$$

In this equation A is the capacity, n is shows the intensity of adsorption. The graph was plotted between log*Ce* vs log*Cads* as shown in Fig 9. The graph shows good correlation coefficient (R^2 0.978) from the slop and intercept the values of A and n can be calculated (Table-2). [33]. The Freundlich capacity value (*A)* indicates that the system is favorable or unfavorable for adsorption process. The value of (*A)* ranges from (1-20 mg/g) is effective for multilayer formation. In this study, the value of A is found above 1 at various temperature and if the sorption intensity value 1 > n > 10 the phenomenon is referred to cooperative in nature whereas, if 1 <n<10 indicates the chemisorption nature. In present study the value of n is 1 <n<10 for Hg^{2+} (Table-2), suggesting chemisorption nature of reaction with good R^2 value indicates the favorability of this model [34]. However, comparing the both models it has observed that the Langmuir model has high value of (R^2 0.999*)* as compared to Freundlich model (R^2 0.988). Therefore, the adsorption takes place by monolayer formation.

Table-2: Fruendlich adsorption isotherm parameters.

Temperature	A (mg g^{-1})	n	R^2
298	1.799	0.81	0.973
303	1.809	0.87	0.980
308	1.811	0.89	0.969

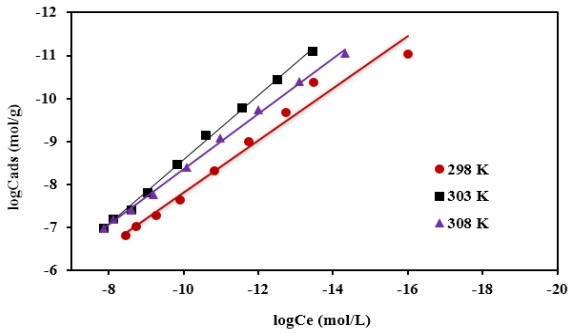

Fig.9: Freundlich isotherm model (Conc. 1×10^{-7} to 1×10^{-4} mol/L, 25 mg/L resin-4 60 min shaking time at 9 pH and 298-308 K).

The (D-R) Dubinin–Radushkevich model describes the adsorption mechanism either chemical or physical. The linear form of DR model is given in (Equation 7).

$$\ln C_{ads} = \ln X_m - \beta\varepsilon^2 \qquad (7)$$

where *Xm* shows adsorption capacity, *ß* is activity coefficient and ε is the Polanyi potential equation, which can be calculated by equation 8.

$$\varepsilon = RT \ln\left(1+\frac{1}{C_e}\right) \qquad (8)$$

where *R* stand for the general gas constant and *T* shows the temperature in Kelvin and *E* (kJ/mol) mean energy which can be calculated by Equation (9).

$$E = \frac{1}{\sqrt{-2\beta}} \qquad (9)$$

The graph has been plotted between the lnCads and ε value which shows the good correlation coefficient (R^2 0.999) presented in Fig 10. From the slop and intercept the value of *Xm* and *ß* have been calculated (Table-3)[32].

Column Adsorption Study

The use of breakthrough curve is very helpful to provide knowledge about dynamic adsorption capacity of column. The saturation of column can be defined by the position of curve which depends upon flow rate and concentration of analyte. Therefore, it is the ratio of inlet to effluent concentration of metal ions as function of time and volume. The conditions which were already optimized during the batch adsorption study were applied and adjusted flow rate at 2 $mLmin^{-1}$. The breakthrough capacity was calculated from the graph in Fig 11, which shows that breakthrough capacity of column was **0.21** mg/L.

Table-3: D-R adsorption isotherm parameters.

Temperature	*Xm*(mmol/g)	*E*(kJ/mol)	R^2
298	0.281	10.09	0.989
303	0.331	11.88	0.990
308	0.491	12.01	0.997

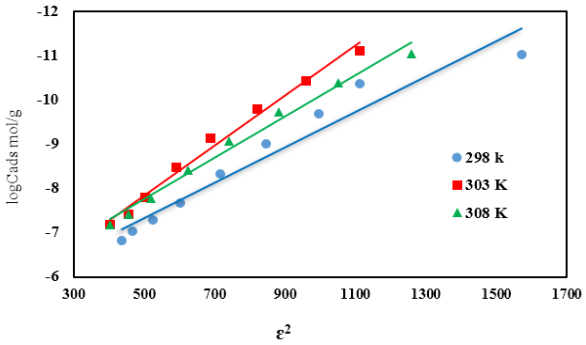

Fig.10: D-R isotherm model (Conc. 1×10^{-7} to 1×10^{-4} mol/L, 25 mg/L resin-4**,** 60 min shaking time at 9 pH and 298 K).

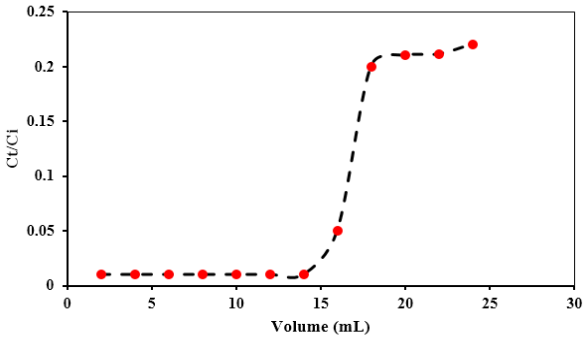

Fig.11: Breakthrough curve of Hg^{2+} ions (Conc. 1x 10^{-4} mol/L at 298 K).

Thomas model

Thomas model describes the dynamic adsorption phenomenon. The column data was analysed by using Thomas model equation (3) to determine (q_o) and (k_{TH}) Thomas rate constant. The graph was plotted between $\ln\left(\frac{C_0}{C}-1\right)$ against t (min) at constant flow rate Fig 12. From the slop and intercept it has found that the maximum solid phase concentration (*qo*) was 7.5 and Thomas model rate constant k_{TH} was found to be 0.176 with (R^2 0.938) for Hg^{2+} ions.

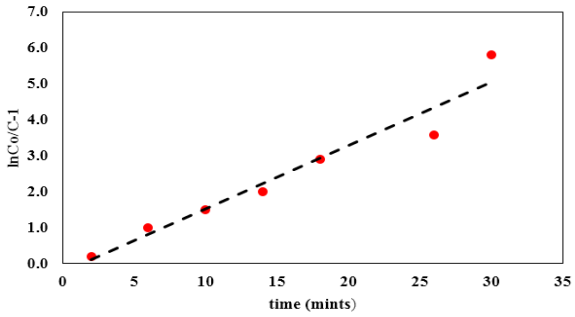

Fig. 12: Thomas model graph of $\ln\left(\frac{C_0}{C}-1\right)$ vs. t for Hg^{2+} ions ($1x10^{-4}$ mol/L at 298 K).

Thermodynamics Study

The temperature has very major role on adsorption process, therefore the adsorption of Hg^{2+} ions have been analyzed at various temperature (298-308 K) shown in Fig 13 to determine the thermodynamic parameters such as Gibbs free energy (ΔG), enthalpy (ΔH) and entropy (ΔS)[35]. The thermodynamic parameters can be calculated using equation 10 and 11:

$$\ln k_c = \frac{-\Delta H}{RT} + \frac{\Delta S}{R} \qquad (10)$$

$$\Delta G = -RT \ln k_c \qquad (11)$$

where R is the gas constant (8.314 J/mol K) and k_c is the equilibrium constant. The graph has been plotted between lnk_c versus $1/T$ Fig 14, from the slop and intercept the values of ΔH (KJ/mol) and ΔS (KJ/mol /K) can be obtained given in Table-4. It has noticed that the values of ΔG are negative which shows that the reaction is spontaneous and increases the negative values with raising of temperature which is thermodynamically favorable process. The positive values of enthalpy ΔH and entropy suggest that the process is endothermic and increases randomness onto resin-4 surface [36].

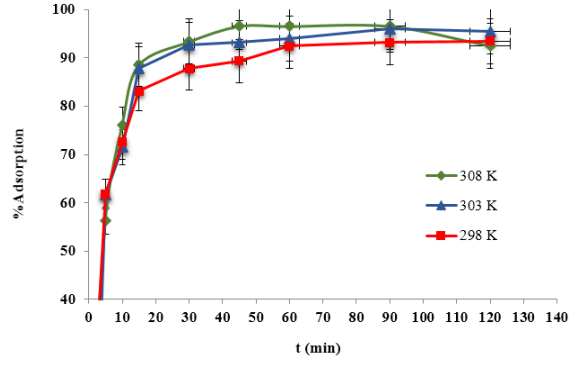

Fig.13: Adsorption of Hg^{2+} ions on resin-4 as a function of different temperatures and time.

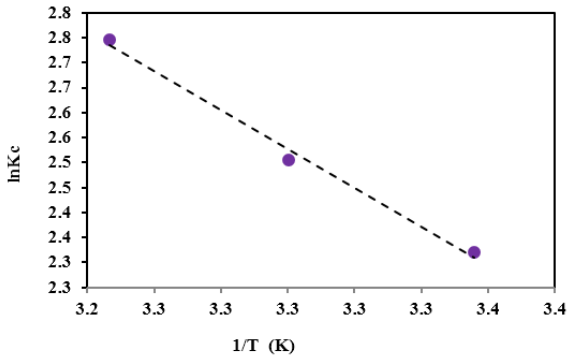

Fig.14: Van't Hoff plot for the adsorption of Hg^{2+} ions onto resin-4.

Kinetic Study

The kinetic study for the adsorption of Hg^{2+} ions onto resin-4 has been performed that describes the pathway of uptake rate of Hg^{2+} ions at different time. Therefore, the adsorption mechanism was investigated by applying the different kinetic models such as pseudo first order and pseudo second order kinetic equations 12 and 13 respectively [37].

$$\log(q_e - q_t) = \ln q_e - k_1 t \qquad (12)$$

$$\frac{t}{q_t} = \left(\frac{t}{k_2 q_e^2}\right) + \left(\frac{1}{q_e}\right) \qquad (13)$$

where the qe and qt shows the amount of Hg^{2+} ions adsorbed (mg/g) at equilibrium and at time t, respectively, while k_1 and k_2 demonstrate the rate constants of the pseudo first and second order respectively.

The experimental data were subject towards the pseudo first order kinetic model by plotting the graph between $\ln(q_e\text{-}q_t)$ vs t as shown in Fig 15. From the slop and intercept the constant values of qe and k were calculated and given in Table 5. It is clear that experimental data follows pseudo first order kinetic with good correlation coefficient value R^2. Moreover, the pseudo second order kinetic model was also applied by plotting the graph between t/q_t vs t Fig 16, from the slop and intercept the constant values of this model were calculated and given in Table 5. It is examined that the data follows pseudo second order kinetic model very well with good correlation coefficient value.

Table-4: Thermodynamic parameters for adsorption of Hg^{2+} ions.

ΔH (KJ/mol)	ΔS (KJ/mol K)	T (K)	ΔG (KJmol)	lnk_c
0.032	0.127	293	-5.747	2.32
		303	-6.306	2.50
		308	-7.027	2.75

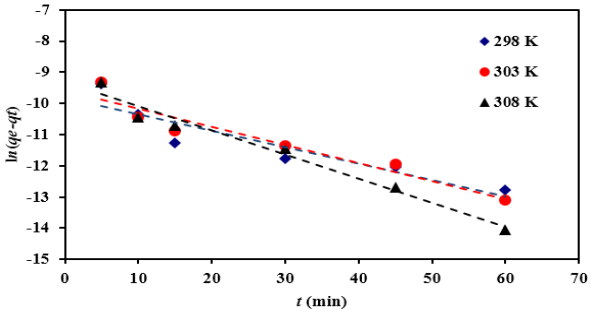

Fig. 15: The pseudo first order kinetic model for the adsorption of Hg^{2+} ions onto resin-4**.**

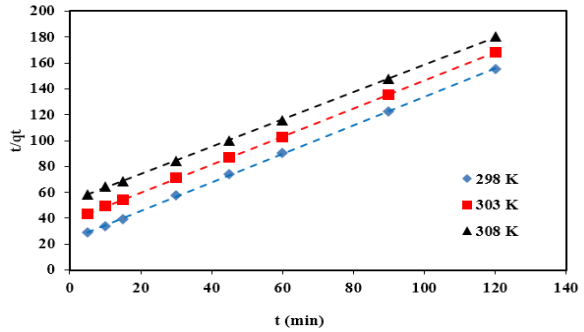

Fig. 16: The pseudo second order kinetic model for the adsorption of Hg^{2+} ions onto resin-4**.**

The Morris– Weber model has been examined onto the experimental data using the following equation 14

$$qt = Rid\sqrt{t} \qquad (14)$$

where qt shows the adsorbed concentration at time t, Rid are the rate constant. Therefore in (Fig 17) the graph have been plotted qt vs $t^{½}$, from the slop value of R*id* was determined which is equal to 0.08 $mol.g^{-1}$ $min^{t-1/2}$ with correlation coefficient of (R^2= 0.980).

Moreover, to check that adsorption mechanism that had happened via film diffusion or intraparticle diffusion the Reichenberg equation has been applied. The linear form Reichenberg equation 15 is given below

$$Q = 1 - \frac{6e^{\beta t}}{\pi^2} \qquad (15)$$

In this equation Q = qt/qm, Bt = π^2 Di/r^2, qt shows the concentration adsorbed at time t. qm is the maximum adsorption capacity of the resin-4 and Di is the effective diffusion coefficient of the adsorbate species inside the sorbent particle. The value of *Bt* which is a mathematical function of Q, determined by using following equation 16:

$$Bt = -0.4977 - \ln(1 - Q) \qquad (16)$$

The plot of Bt versus time (Fig 17) follows linearity from 0 to 60 min, which indicates that the intraparticle diffusion is the rate controlling step with a small friction of sorption that occurs through film diffusion because the plot does not pass through origin.

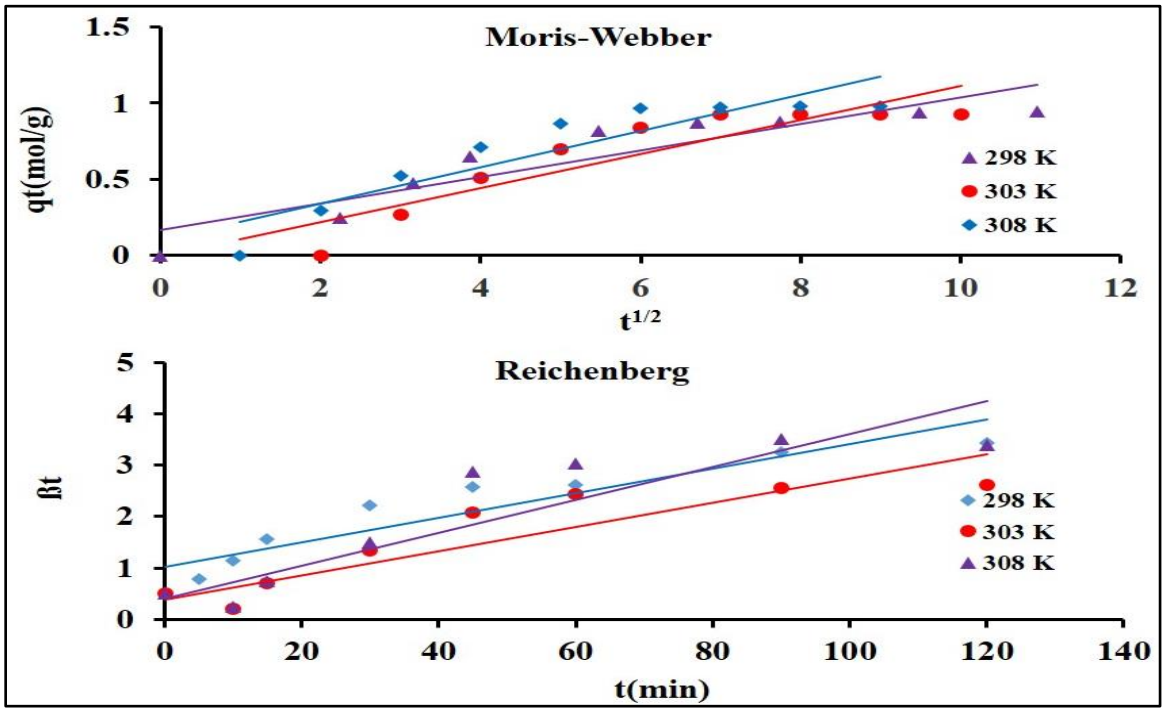

Fig. 17: Reichenberg and Mors Webber graphs for Hg^{2+} ions at different temperatures.

Table-5: Pseudo first and second order kinetic table for the Hg^{2+} ion.

Temperature	Pseudo-first order kinetic model			Pseudo-second order kinetic model		
	K_1 min^{-1}	q_e $mmolg^{-1}$	R^2	K_2 g $mol^{-1}min^{-1}$	q_e $molg^{-1}$	R^2
298	0.24	0.781	0.978	118.7	0.227	0.999
303	0.46	0.893	0.908	154.6	0.302	0.999
308	0.58	0.889	0.971	251.6	0. 414	0.999

Reusability Study

The resin-4 was reused many times by washing with 0.01 M NaOH solution. The results show that the resin-4 can be recycled up to 15 times without any loss in adsorption efficiency. After 15 times resin-4 shows 1.2 less % adsorption because during the recycling and washing some amount of resin has been lost by handling as shown in Fig 18a. The stability of resin-4 after recycling was confirmed by FTI-R and SEM techniques mentioned in Fig 18b which clearly demonstrate the stability of resin-4 after using many times.

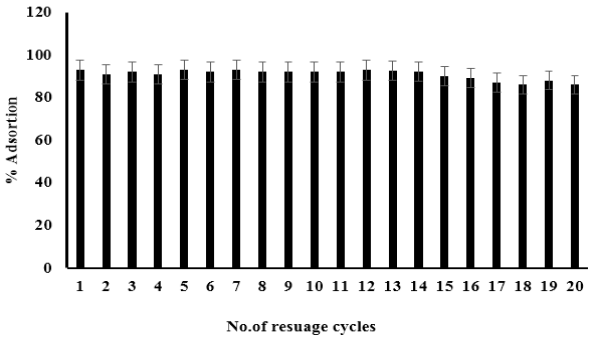

Fig. 18: (a) The reusability of resin-4 for the adsorption of Hg^{2+} ions.

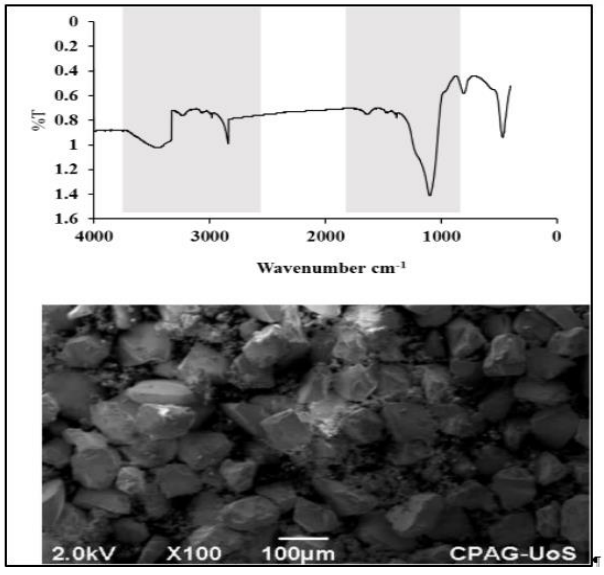

Fig.18: (b) The FT-IR and SEM images of resin-4after removal of Hg^{2+} ions.

Real Wastewater Samples

The Hg^{2+} contaminated wastewater samples were collected from local industrial zone and added 25 mg of resin-4. The concentrations of Hg^{2+} ions were determined before and after adding the resin-4 (Table **6)**. The results demonstrates that the resin-4 is most effective material for the decontamination of Hg^{2+} ions.

Table-6: Adsorption Hg^{2+} ions from real wastewater samples

Sample. No	Conc.(mol.L-1) before	Conc. (mol.L-1) after	% Adsorption
1	1.00×10^{-5}	1.00×10^{-8}	99.989
2	2.90×10^{-6}	3.78×10^{-7}	86.965
3	1.70×10^{-6}	2.50×10^{-7}	85.294

Interference Study

Mostly the industrial wastewater contains many other ionic species which may interfere with the uptake of targeted analyte. The study has been performed under the influences of different coexisting interfering ions with different ratios such as 1:1, 1:5 and 1:10. Results show that there is no significant change has been observed in % adsorption of mercury metal ions shown in Fig. 19.

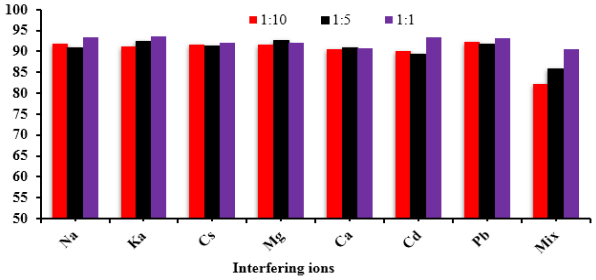

Fig. 19: The adsorption of Hg^{2+} ions on resin-4 in the presences of other ions.

Comparative Study

The adsorption efficiency of resin-4 was compared with already published adsorbent material for the adsorption of Hg^{2+} ions given in table 7. The results show that the adsorption efficiency and selectivity of resin-4 is relatively better as compared to the other materials.

Table-7: The comparison of resin-4 with other adsorbent material.

Adsorbent	Adsorbate	Adsorbent amount	% Adsorption /Adsorption capacity	References
Piperdinomethylcalix[4]arene silica resin	Cu^{2+}, Pb^{2+}	**30 mg**	**90%**	**[26]**
Diethylamine calix[4]arene silica resin	Cd^{2+}, Pb^{2+}, Hg^{2+}	**0.1 g**	**98%**	**[27]**
Thioether-Crown-Rich Calix[4]arene Porous Polymer	Hg^{2+}	**20 mg**	**98%**	**[38]**
Hybrid Clay/Calix[4]arene	Cd^{2+}	**300 mg**	**92.8%**	**[39]**
Diphenylamine calix[4]arene based silica resin-4	Hg^{2+}	**25mg**	**92.9%**	**Present study**

Conclusion

This study is related with the synthesis of *p*-diphenylaminomethylcalix[4]arene based resin for the removal of Hg^{2+} ion from water. The synthesized resin-4 was applied for the selective removal of Hg^{2+} ion under the optimized conditions. The experimental data was subjected to different isotherm models and the Langmuir isotherm model was found to be the best-fit for Hg^{2+} ions. However, mean free energy of sorption from the D-R isotherm, was calculated as (10.09-12.01) kJ/mol for Hg^{2+} ions, besides this, the thermodynamic and kinetic study shows the feasibility and mechanism of adsorption process. Hopefully this study will finds its applicability in industries.

Acknowledgement

We are thankful to the National Centre of Excellence in Analytical Chemistry, University of Sindh Jamshoro for the their kind support for this work

References

1. G. Lin, C. Wang, X. Li, Y. Xi, W. Wang, L. Zhang, and J.Chang, Synthesis of coordination polymer by 2, 2′-dithiodipropionic acid and selective removal of Hg (ii)/Pb (ii) in wastewater, *J Taiwan Inst Chem Eng*., **113**, 315 (2020).
2. H. A. Elbadawy, Adsorption and structural study of the chelating resin, 1, 8-(3, 6-dithiaoctyl)-4-polyvinyl benzenesulphonate (dpvbs) performance towards aqueous Hg (II), *J. Mol. Liq.*, **277**, 584 (2019).
3. M. R. Awual, M. M. Hasan, G. E. Eldesoky, M. A. Khaleque, M. M. Rahman, and M. Naushad, Facile mercury detection and removal from aqueous media involving ligand impregnated conjugate nanomaterials, *Chem. Eng. J.*, **290**, 243 (2016).
4. M. Naushad, Surfactant assisted nano-composite cation exchanger: development, characterization and applications for the removal of toxic Pb^{2+} from aqueous medium, *Chem. Eng. J.*, **235**, 100 (2014).
5. P. Ahmad, M. A. Ahanger, D. Egamberdieva, P. Alam, M. N. Alyemeni, and M. Ashraf, Modification of osmolytes and antioxidant enzymes by 24-epibrassinolide in chickpea seedlings under mercury (Hg) toxicity, *J. Plant Growth Regu*l., **37**, 309 (2018).
6. A. Jamshaid, A. Hamid, N. Muhammad, A. Naseer, M. Ghauri, J. Iqbal, S. Rafiq, and N.S. Shah, , Cellulose-based Materials for the Removal of Heavy Metals from Wastewater–An Overview, *ChemBioEng Rev*., **4**, 240 (2017).
7. A. Qayoom, S. A. Kazmi, and S. N. Ali, Kinetic Modelling of Aqueous Copper (II) Ions Adsorption onto Turmeric Powder: Effect of Temperature, *J. Chem. Soc. Pak.*, **39**, (2017).
8. R. M. Aishah, J. Shamshuddin, C. I. Fauziah, A. Arifin, and Q. A. Panhwar, Adsorption-desorption characteristics of zinc and copper in oxisol and ultisol amended with sewage sludge, *J. Chem. Soc. Pak.*, **40**, 842, (2018).
9. S. Zhu, B. Chen, M. He, T. Huang, and B. Hu, Speciation of mercury in water and fish samples by HPLC-ICP-MS after magnetic solid phase extraction, *Talanta*, **171**, 213 (2017).
10. A. Fashi, M. R. Yaftian, and A. Zamani, Electromembrane extraction-preconcentration followed by microvolume UV–Vis spectrophotometric determination of mercury in water and fish samples, *Food Chem*., **221**, 714 (2017).
11. S. A. Ali and M. A. Mazumder, A new resin embedded with chelating motifs of biogenic methionine for the removal of Hg (II) at ppb levels, *J. Hazard. Mater.*, **350**, 169 (2018).
12. M. Naushad, Z. Alothman, M. R. Awual, M. M. Alam, and G. Eldesoky, Adsorption kinetics, isotherms, and thermodynamic studies for the adsorption of Pb^{2+} and Hg^{2+} metal ions from aqueous medium using Ti (IV) iodovanadate cation exchanger, *Ionics*, **21**, 2237 (2015).
13. M. Naushad, S. Vasudevan, G. Sharma, A. Kumar, and Z. Alothman, Adsorption kinetics, isotherms, and thermodynamic studies for Hg^{2+} adsorption from aqueous medium using alizarin red-S-loaded amberlite IRA-400 resin, *Desalination Water Treat.*, **57**, 18551 (2016).
14. A. Parchebaf and G. Nojameh, Modified nano-γ-alumina with 2, 4-dinitrophenyl hydrazine as an efficient adsorbent for the removal of everzol red 3BS dye from aqueous solutions, *Eurasian Chemical Communications*, **2,** 475 (2020).
15. H. Shahzad, R. Ahmadi, J. Najafpour, and F. Adhami, Adsorption of Cytarabine on the Surface of Fullerene C20: A Comprehensive DFT Study, *Eurasian Chemical Communications*, **2**, 162, (2020).

16. E. Fereydoun Asl, F. S. Mohseni-Shahri, and F. Moeinpour, $NiFe_2O_4$ coated sand as a nano-adsorbent for removal of Pb (II) from aqueous solutions, *Eurasian Chemical Communications*, **1**, 480 (2019).
17. M. Janighorban, N. Rasouli, N. Sohrabi, and M. Ghaedi, Response Surface Methodology for Optimizing Cd(II) Adsorption onto a Novel Chemically Changed Nano Zn_2Al-Layer Double Hydroxide, *Advanced Journal of Chemistry-Section A.*, **3**, 701 (2020).
18. M. R. Mirbaloochzehi, A. Rezvani, A. Samimi, and M. Shayesteh, Application of a Novel Surfactant-Modified Natural Nano-Zeolite for Removal of Heavy Metals from Drinking Water, *Advanced Journal of Chemistry-Section A.*, ***3***, 612 (2020).
19. P. K. Jal, S. Patel, and B. K. Mishra, Chemical modification of silica surface by immobilization of functional groups for extractive concentration of metal ions, *Talanta*, **62**, 1005, (2004).
20. A. M. Starvin, Ph.D. Thesis, Offline and online solid phase extraction/preconcentration of inorganics, Cochin University of Science and Technology, (2005).
21. R. Junejo, S. Memon, and S. Kaya, Effective Removal of the Direct Black-38 Dye from Wastewater Using a New Silica-Modified Resin: Equilibrium and Thermodynamics Modeling Studies, *J. Chem. Eng. Data.*, **65**, 4805, (2020).
22. H. R. Nodeh, M. A. Kamboh, W. A. W. Ibrahim, B. H. Jume, H. Sereshti, and M. M. Sanagi, Equilibrium, kinetic and thermodynamic study of pesticides removal from water using novel glucamine-calix [4] arene functionalized magnetic graphene oxide, *Environ Sci Process Impacts*., **21**, 714 (2019).
23. M. A. Kamboh, W. A. Wan Ibrahim, H. Rashidi Nodeh, L. A. Zardari, S. T. H. Sherazi, and M. M. Sanagi, p-Sulphonatocalix [8] arene functionalized silica resin for the enhanced removal of methylene blue from wastewater: equilibrium and kinetic study, *Sep Sci Technol*., **54**, 2240, (2019).
24. R. Junejo, N. S. Jalbani, S. Memon, S. Kaya, S. Erkan, G. l. Serdaroğlu, and I.M. Palabiyik, Equilibrium, Thermodynamic, and Density Functional Theory Modeling Studies for the Removal of Dichromate Ions from Wastewater Using Calix [4] arene Modified Silica Resin, J. Chem. Eng. Data., ***66***, 1,379, (2020).
25. S. Sultan, A. Shah, B. Khan, J. Nisar, M. R. Shah, M. N. Ashiq, M.S. Akhter, and A.H. Shah, Calix [4] arene Derivative-Modified Glassy Carbon Electrode: A New Sensing Platform for Rapid, Simultaneous, and Picomolar Detection of Zn (II), Pb (II), As (III), and Hg (II), *ACS omega*, **4**, 16860 (2019).
26. R. Junejo, S. Memon, F. Durmaz, A. A. Ahmed, F. N. Memon, N. S. Jalbani, S.S. Memon, and A.A. Bhatti, Synthesis of Piperdinomethylcalix[4]arene Attached Silica Resin for the Removal of Metal Ions from Water: Equilibrium, Thermodynamic and Kinetic Modelling Studies, *Advanced Journal of Chemistry-Section A.*, **3**, 680, (2020).
27. R. Junejo, S. Memon, and I. M. Palabiyik, Efficient adsorption of heavy metal ions onto diethylamine functionalized calix[4]arene based silica resin, Eurasian Chemical Communications, **2**, 785, 2020.
28. C. D. Gutsche, M. Iqbal, and D. Stewart, Calixarenes. 19. Syntheses procedures for p-tert-butylcalix [4] arene, *J. Org. Chem.*, **51**, 742, 1986.
29. R.G. Pearson, Hard and soft acids and bases, *J. Am. Chem. Soc.*, **85**, 3533, 1963.
30. R. Junejo, S. Memon, F. Durmaz, A. A. Ahmed, F. N. Memon, N. S. Jalbani, S.S. Memon, and A.A. Bhatti, Synthesis of Piperdinomethylcalix[4]arene Attached Silica Resin for the Removal of Metal Ions from Water: Equilibrium, Thermodynamic and Kinetic Modelling Studies, *Advanced Journal of Chemistry-Section A.*, (2020).
31. R. Junejo, S. Memon, F. N. Memon, A. A. Memon, F. Durmaz, A. A. Bhatti, and A.A. Bhatti, Thermodynamic and Kinetic Studies for Adsorption of Reactive Blue (RB-19) Dye Using Calix [4] arene-Based Adsorbent, *J. Chem. Eng. Data*, **64**, 3407, (2019).
32. F. Batool, J. Akbar, S. Iqbal, S. Noreen, and S. N. A. Bukhari, Study of isothermal, kinetic, and thermodynamic parameters for adsorption of cadmium: an overview of linear and nonlinear approach and error analysis, *Bioinorg Chem Appl*, (2018).
33. Y. Satlaoui, R. Nasraoui, A. Charef, and R. Azouzi, Adsorption, Modeling, Thermodynamic, and Kinetic Studies of Methyl Red Removal from Textile-Polluted Water Using Natural and Purified Organic Matter Rich Clays as Low-Cost Adsorbent, *J. Chem*, (2020).
34. H. Wang, Z. Li, S. Yahyaoui, H. Hanafy, M. K. Seliem, A. Bonilla-Petriciolet, G.L. Dotto, L. Sellaoui, and Q. Li, Effective adsorption of dyes on an activated carbon prepared from carboxymethyl cellulose: Experiments, characterization and advanced modelling, *Chem. Eng. J.*, **417,** 128116, (2020).
35. D. K. Singh, S. Mohan, V. Kumar, and S. H. Hasan, Kinetic, isotherm and thermodynamic studies of adsorption behaviour of CNT/CuO nanocomposite for the removal of As (III) and As (V) from water, RSC advances, **6**, 1218, (2016).

36. E. A. Ofudje, I. A. Adeogun, M. A. Idowu, S. O. Kareem, and N. A. Ndukwe, Simultaneous removals of cadmium (II) ions and reactive yellow 4 dye from aqueous solution by bone meal-derived apatite: kinetics, equilibrium and thermodynamic evaluations, *J Anal Sci Technol*, **11**, 1, (2020).
37. U. A. Edet and A. O. Ifelebuegu, Kinetics, Isotherms, and Thermodynamic Modeling of the Adsorption of Phosphates from Model Wastewater Using Recycled Brick Waste, Processes, **8**, 665, (2020).
38. D. Shetty, S. Boutros, A. Eskhan, A. M. De Lena, T. Skorjanc, Z. Asfari, H.Traboulsi, J. Mazher, J. Raya, F. Banat, and A. Trabolsi, Thioether-crown-rich calix [4] arene porous polymer for highly efficient removal of mercury from water, *ACS Appl. Mater. Interfaces*, **11**, 12898, (2019).
39. K. Jlassi, K. Eid, M. H. Sliem, A. M. Abdullah, and M. M. Chehimi, Calix [4] arene-clicked clay through thiol-yne addition for the molecular recognition and removal of Cd (II) from wastewater, *Sep. Purif. Technol*, **251**, 117383, (2020).